Electronic Supporting Information

Cell organelle targeting of near-infrared croconaine dye controls photothermal outcome

Ying Wen, Hannah H. McGarraugh, Cynthia L. Schreiber, and Bradley D. Smith*

[a] Department of Chemistry and Biochemistry, 251 Nieuwland Science Hall, University of Notre Dame, Notre Dame, Indiana 46556, USA
[b] Institute of Molecular Science, Shanxi University, Taiyuan, 030006, China
*E-mail: smith.115@nd.edu

Contents

1. Experimental Section

Materials. All chemicals and solvents were purchased as reagent grade and used without further purification unless otherwise noted. Calcein AM and Lysotracker Yellow HCK-123 were purchased from Invitrogen. Acridine orange was obtained from Sigma-Aldrich. PSVue643 was purchased from Molecular Targeting Technologies Incorporated. Fetal bovine serum and penicillin/streptomycin were obtained from Atlanta Biologicals and Corning, respectively. Kaighn's Modification of Ham's F-12 Medium (F-12K; ATCC-30-2004) and Eagle's Minimum Essential Medium (EMEM; ATCC-30-2003) were purchased from American Tissue Culture Collection.

Instruments. ^{1}H NMR spectra were recorded on Bruker AVANCE III HD 400 MHz spectrometer at 25 °C. Chemical shift was presented in ppm and referenced by residual solvent peak. High resolution mass spectrometry (HR-MS) was performed using a Bruker micro TOP II spectrometer or AB SCIEX TripleTOF 5600 instrument. Absorption spectra were collected on Evolution 201 UV/Vis Spectrometer with ThermoInsight software. Fluorescence spectra were acquired using a Horiba Fluoromax-4 Fluorometer with FluorEssence software. The cell imaging was performed by Zeiss Axiovert 100 TV epifluorescence microscope equipped with UV filter (ex. 387/11 nm, em. 447/60 nm; blue channel), FITC filter (ex. 450/90 nm, em. 500/50 nm; green channel) and TxRed filter (ex. 562/40 nm, em. 624/40 nm; red channel) and Cy5.5 filter (ex. 655/40 nm, em. 716/40 nm; deep red channel). Fluorescence images were analyzed using ImageJ software. The change in solution temperature was monitored in real time using a USB calibrated thermal video camera (Infrared Cameras Inc, 7320) and confirmed using an Omega hypodermic thermocouple (HYPO-33–31T-G-60-SMPW-M), under irradiation by a continuous wave diode laser (L808P1WJ, 808 nm).

Cell culture. Chinese hamster ovary (CHO-K1, purchased from ATCC: CCL-61) cells were cultured and maintained in F-12K medium (supplemented with 10% fetal bovine serum and 1% penicillin/streptomycin) at 37 °C and 5% CO_2 in a humidified incubator. Human mammary adenocarcinoma (MCF-7, purchased from ATCC: CVCL_0031) were cultured in EMEM medium supplemented with 10% fetal bovine serum, 1% non-essential amino acids, 2% sodium bicarbonate, 1% sodium pyruvate, and 1% penicillin/streptomycin.

Fluorescence Colocalization Studies. MCF-7 or CHO-K1 cells were seeded into 8-well chambered coverglass. For nucleus-targeted probes, on the following day, the cells were incubated with 10 μM **NucCR** or **NucCR'** in Opti-MEM at 37 °C, 5% CO_2. After 2 h, the cells were washed three times with DPBS, fixed with 4% cold paraformaldehyde for 20 min at room temperature, washed once with DPBS, and co-stained with 3 μM Hoechst 33342 for 10 min. Afterwards, the cells were washed two times and imaged on Zeiss fluorescence microscope with UV filter (blue channel) and FITC filter (green channel).

For lysosome-targeted dyes, the cells seeded in 8-well chambered coverglass were incubated with 10 μM **LysoSQ** in Opti-MEM for 2 h at 37 °C, 5% CO_2. Then, the cells were washed two times with DPBS, and stained with 5 μM Lysotracker Yellow for 30 min at 37 °C, 5% CO_2. Afterwards, the cells were washed two times and imaged under Opti-MEM on Zeiss fluorescence microscope with FITC filter (green channel) and Cy5.5 filter (deep red channel).

Photothermal-Induced Cell Death Monitored by MTT Cell Viability Assay. MCF-7 cells were seeded into 384-microwell plates and grown to 70% confluency. The cells were incubated with **NucCR**, **NucCR'** or **LysoCR** at various concentrations (N =3) in Opti-MEM for 2 h at 37 °C, 5% CO_2. The medium was then removed, washed once with DPBS, and replaced with fresh EMEM medium. The microwell plate was placed in a heating chamber and thermally equilibrated to 37 °C. Laser diode at 808 nm (200 mW, 5 W/cm^2, 10 min) was used for cells of the phototherapy group. Then cells were further

cultured in the dark at 37 °C. After 72 h, the medium was removed and replaced with EMEM medium containing [3-(4,5-dimethylthiazol-2-yl)-2,5-diphenyltetrazolium bromide] (MTT, 5 μg/mL). The samples were incubated for 12 h at 37 °C and 5% CO_2 and an SDS-HCl detergent solution was the added. The samples were incubated overnight, and the absorbance of each well was measured at 590 nm (N = 3), where the readings were normalized relative to untreated cells.

Imaging Photothermal-Induced Cell Death Using Fluorescent Live and Dead Cell Stains. MCF-7 cells were seeded into 384-microwell plates and grown to 70% confluency. The cells were incubated with **NucCR** or **NucCR'** at various concentrations (N =3) in Opti-MEM for 2 h at 37 °C, 5% CO_2. The supernatant was removed and the cells were washed once with DPBS and replaced with fresh EMEM medium. Phototherapy groups were irradiated with an 808 nm laser beam (5 W/cm^2) for 10 min. After 48 h, each well was treated with a binary mixture of green fluorescent live-cell stain Calcein AM (3 μg/mL) and red fluorescent dead-cell stain PSVue643 (10 μM) and allowed to stand for 20 min. The cells were washed two times with DPBS and resuspended in Opti-MEM. Cells were imaged on Zeiss fluorescence microscope with FITC filter (green channel) and Cy5.5 filter (deep red channel).

Lysosome Membrane Permeabilization Using Fluorescence Imaging Studies. MCF-7 cells were seeded in the 8-well chambered coverglass and co-incubated with **LysoSQ** (10 μM), **LysoCR** (100 μM) and Hoechst 33342 (3 μM) in Opti-MEM for 2 h. Then, dyes were removed and cells were washed two times with DPBS. After addition with Opti-MEM, cells were imaged on fluorescence microscope with UV filter (blue channel) and Cy5.5 filter (deep red channel).

To evaluate the integrity of lysosomes upon light irradiation, the acridine orange staining assay was carried out. MCF-7 cells, seeded in the 8-well chambered coverglass, were first incubated with **LysoCR** (100 μM, in Opti-MEM) for 2 h, and then the medium were replaced by acridine orange solutions (1 μg/mL in Opti-MEM) with further incubation for 10 min, followed by DPBS washing two times and finally fresh Opti-MEM was added. Laser (808 nm, 5 W/cm^2) irradiation for 10 min was followed by fluorescence microcopy with FITC filter (green channel) and TxRed filter (red channel).

2. Synthesis and Characterization.

PB09 was synthesized according to our previous literature method.[S1]

EtSQ700 was synthesized according to our previous literature method.[S2]

Synthesis of NucCR and NucCR'. The peptide (designated as **pep1** or **pep2**) was synthesized on a solid-phase synthesizer by Bankpeptide Biological Technology Co., Ltd., and modified with **FITC** and 6-azido-norleucine. Copper catalyzed alkyne azide cycloaddition reactions between **pep1/pep2** and **PB09** were performed as reported before. [S3] Each probe was isolated using preparative HPLC**.**

HR-MS: **pep1**, calcd. for $C_{73}H_{114}N_{20}O_{15}S^{4+}$, $[M+6H]^{4+}$ 385.7123, found 385.7119; calcd. for $C_{73}H_{113}N_{20}O_{15}S^{3+}$, $[M+5H]^{3+}$ 513.9472, found 513.9468; calcd. for $C_{73}H_{112}N_{20}O_{15}S^{2+}$, $[M+4H]^{2+}$ 770.4169, found 770.4162.

HR-MS: **pep2**, calcd. for $C_{79}H_{126}N_{22}O_{16}S^{4+}$, $[M+6H]^{4+}$ 417.7361, found 417.7359; calcd. for $C_{79}H_{125}N_{22}O_{16}S^{3+}$, $[M+5H]^{3+}$ 556.6455, found 556.6453; calcd. for $C_{79}H_{124}N_{22}O_{16}S^{2+}$, $[M+4H]^{2+}$ 834.4643, found 834.4637.

HR-MS: **NucCR**, calcd. for $C_{100}H_{140}N_{22}O_{20}S_3^{2+}$, $[M+4H]^{2+}$ 1032.4888, found 1032.4869; calcd. for $C_{100}H_{142}N_{22}O_{20}S_3^{4+}$, $[M+6H]^{4+}$ 516.7483, found 516.7479; calcd. for $C_{100}H_{143}N_{22}O_{20}S_3^{5+}$, $[M+7H]^{5+}$ 413.6002, found 413.5997.

HR-MS: **NucCR'**, calcd. for $C_{106}H_{152}N_{24}O_{21}S_3^{2+}$, $[M+4H]^{2+}$ 1096.5363, found 1097.5366; calcd. for $C_{106}H_{153}N_{24}O_{21}S_3^{3+}$, $[M+5H]^{3+}$ 731.3601, found 731.3589; calcd. for $C_{106}H_{154}N_{24}O_{21}S_3^{4+}$, $[M+6H]^{4+}$

548.7721, found 548.7717; calcd. For $C_{106}H_{155}N_{24}O_{21}S_3^{5+}$, $[M+7H]^{5+}$ 439.2192, found 439.2189.

Synthesis of LysoCR. The croconaine **PB09**, 4-(3-azidopropyl)morpholine (16.4 mg), CuTBTABr (5.2 mg), and triethylamine (22 μL) were combined in 5 mL of chloroform and stirred at room temperature overnight. The solution was evaporated and the residue purified by silica column (0-20% MeOH in $CHCl_3$ to give the product as a brown solid (31.5 mg, 95%). δH (400 MHz; $CDCl_3$; Me_4Si) 1.18 (6 H, br t, 4-H), 1.97 (4H, m, 10-H), 2.24 (4H, m, 11-H), 2.31 (8H, br s, 12-H), 3.60 (4H, br m,5-H, 3-H), 3.70 (8H, br t, 13-H), 3.77 (4H, br t, 6-H), 4.34 (4H, t, $J_{9,10}$ 7.0 Hz, 9-H), 4.58 (4H, s, 7-H), 6.44 (2H, m, 2-H), 7.46 (2H, m, 8-H), 8.66 (2H, m, 1-H); ESI m/z 865.3848 $[M+H]^+$ $C_{41}H_{57}N_{10}O_7S_2$ (calcd. 865.3844).

Synthesis of LysoSQ. The squaraine **EtSQ700** (16 mg), 4-(3-azidopropyl)morpholine (13.7 mg), CuTBTABr (4.3 mg), and triethylamine (18 μL) were combined in 5 mL of chloroform and stirred at room temperature overnight. The solution was evaporated and the residue purified by silica column (0-20% MeOH in $CHCl_3$) to give the product as a blue solid (11.6 mg, 43%). δH (400 MHz; $CDCl_3$; Me_4Si) 1.21 (6 H, br t, 4-H), 1.98 (4H, m, 10-H), 2.26 (4H, t, $J_{11,10}$ 6.8 Hz, 11-H), 2.32 (8H, br s, 12-H), 3.49 (4H, q, $J_{3,4}$ 7.2 Hz, 3-H), 3.59 (4H, t, $J_{5,6}$ 5.2 Hz,5-H), 3.62 (8H, t, $J_{13,12}$ 4.7 Hz, 13-H), 3.73 (4H, t, $J_{6,5}$ 5.2 Hz, 6-H), 4.35 (4H, t, $J_{9,10}$ 7.1 Hz, 9-H), 4.58 (4H, s, 7-H), 6.19 (2H, d, $J_{2,1}$ 4.7 Hz, 2-H), 7.44 (2H, s, 8-H), 7.87 (2H, d, $J_{1,2}$4.7 Hz, 1-H); ESI m/z 837.3898 [M+H]+ $C_{40}H_{57}N_{10}O_6S_2$ (calcd. 837.3890).

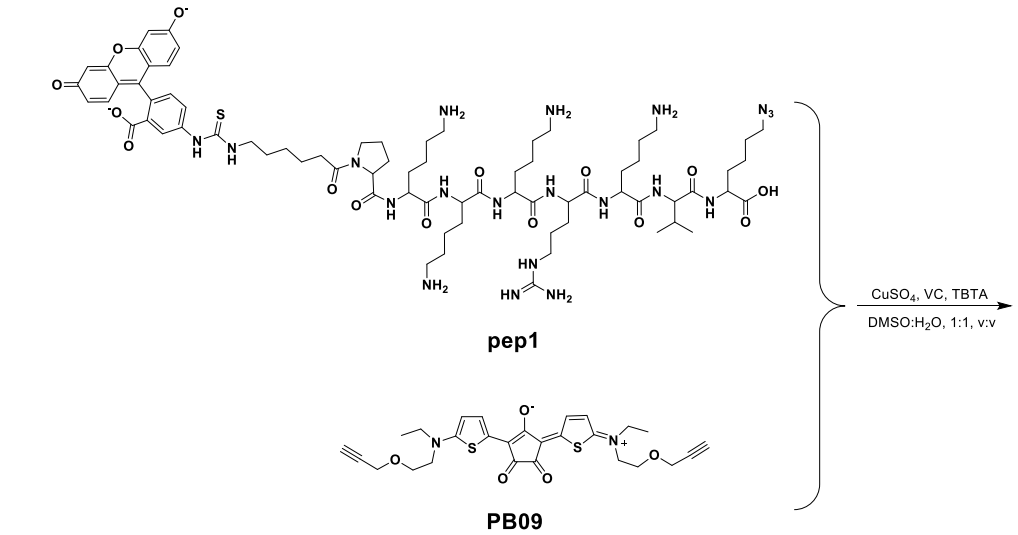

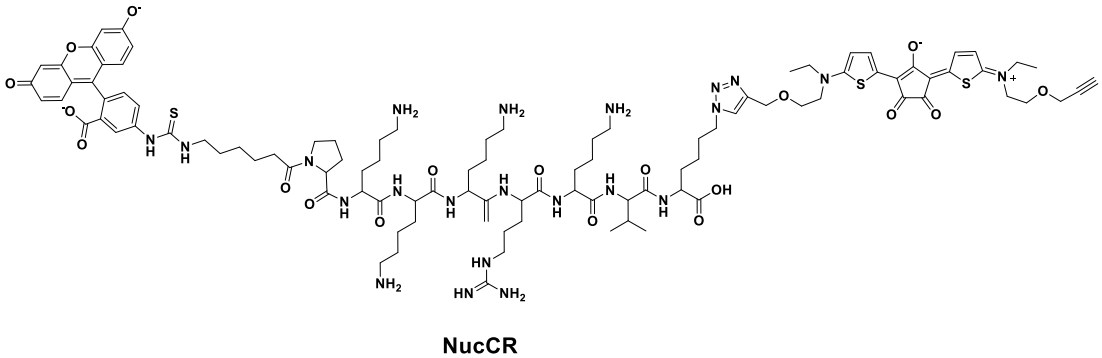

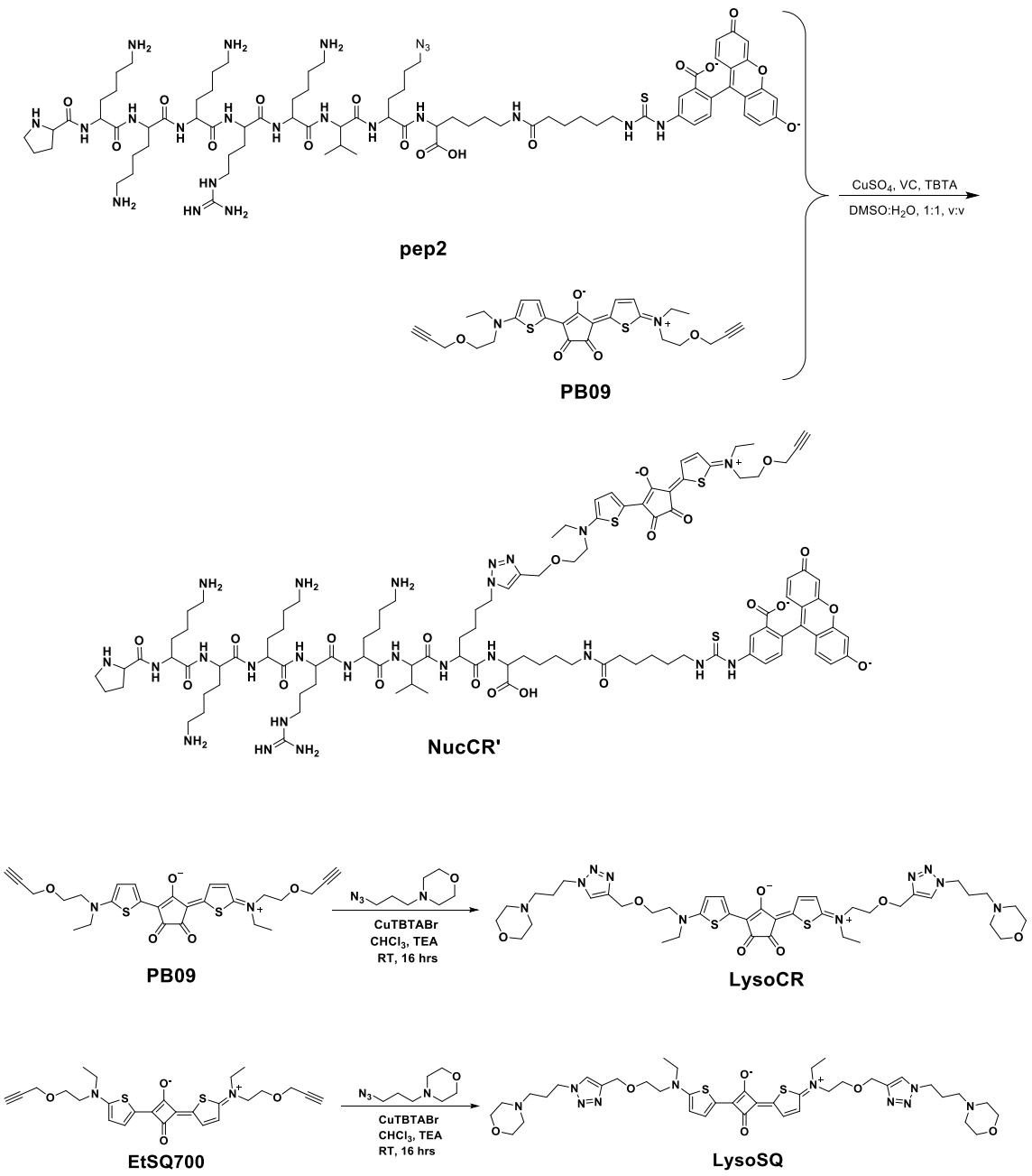

Scheme S1. The synthetic routes of **NucCR**, **NucCR'**, **LysoCR** and **LysoSQ.**

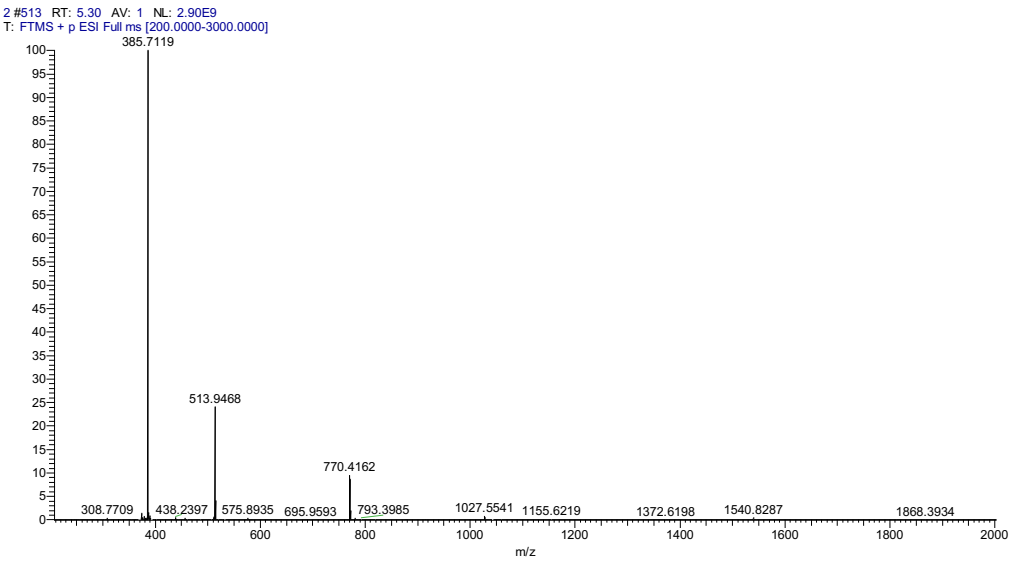

Figure S1. The HR-MS of **pep1**.

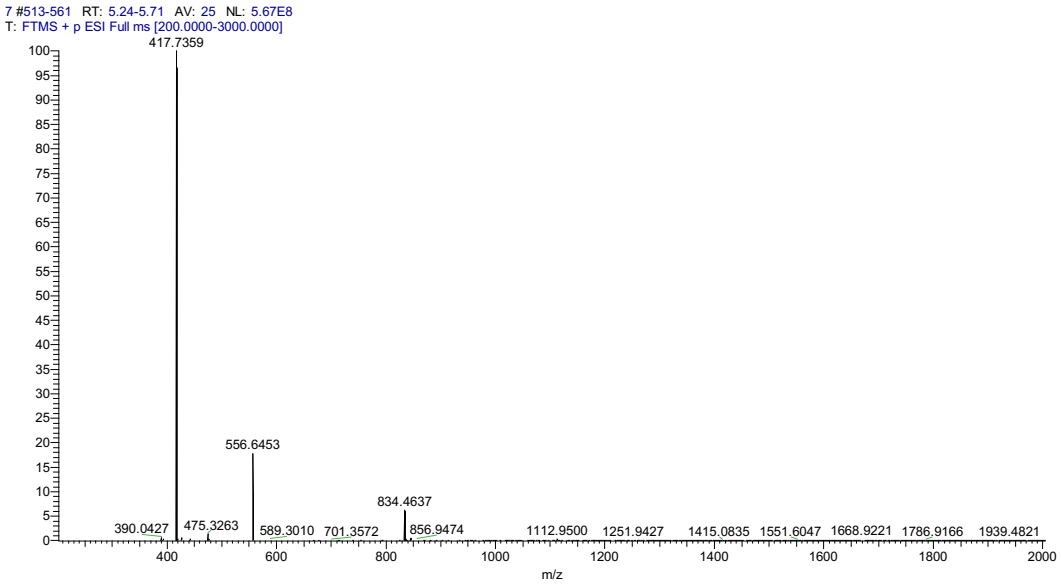

Figure S2. HR-MS of **pep2**.

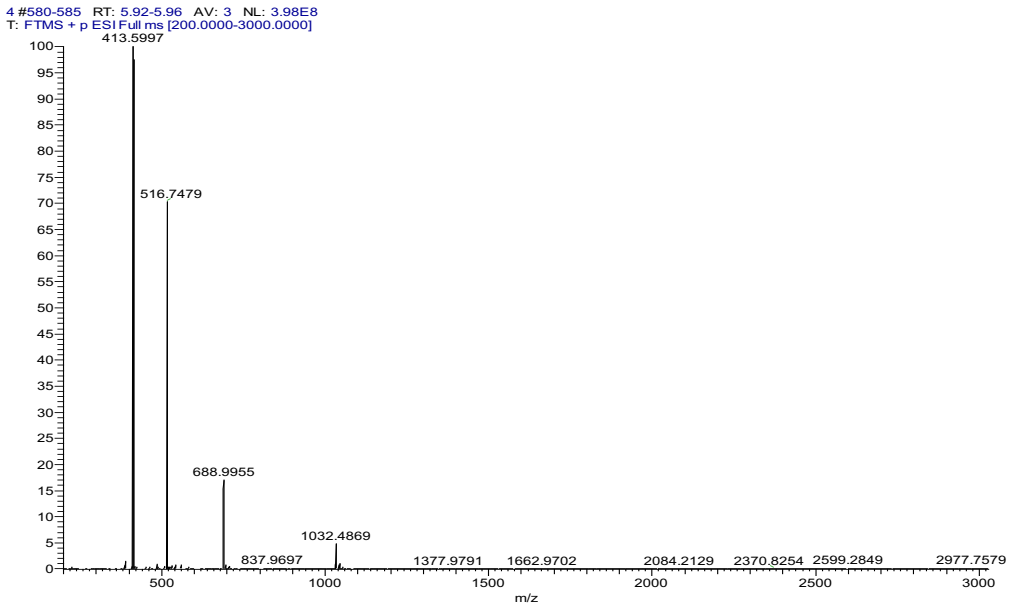

Figure S3. HR-MS of **NucCR**.

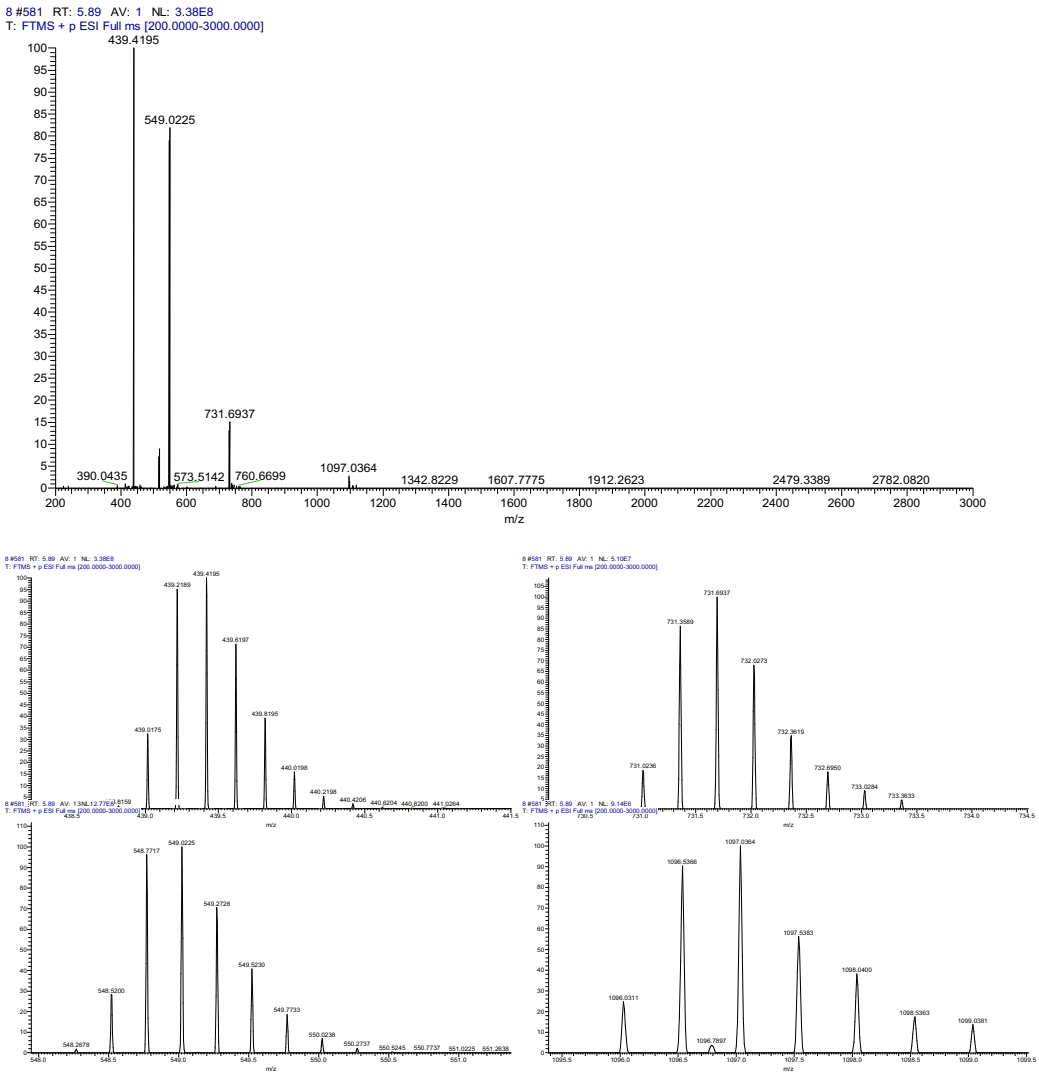

Figure S4. HR-MS of **NucCR'**.

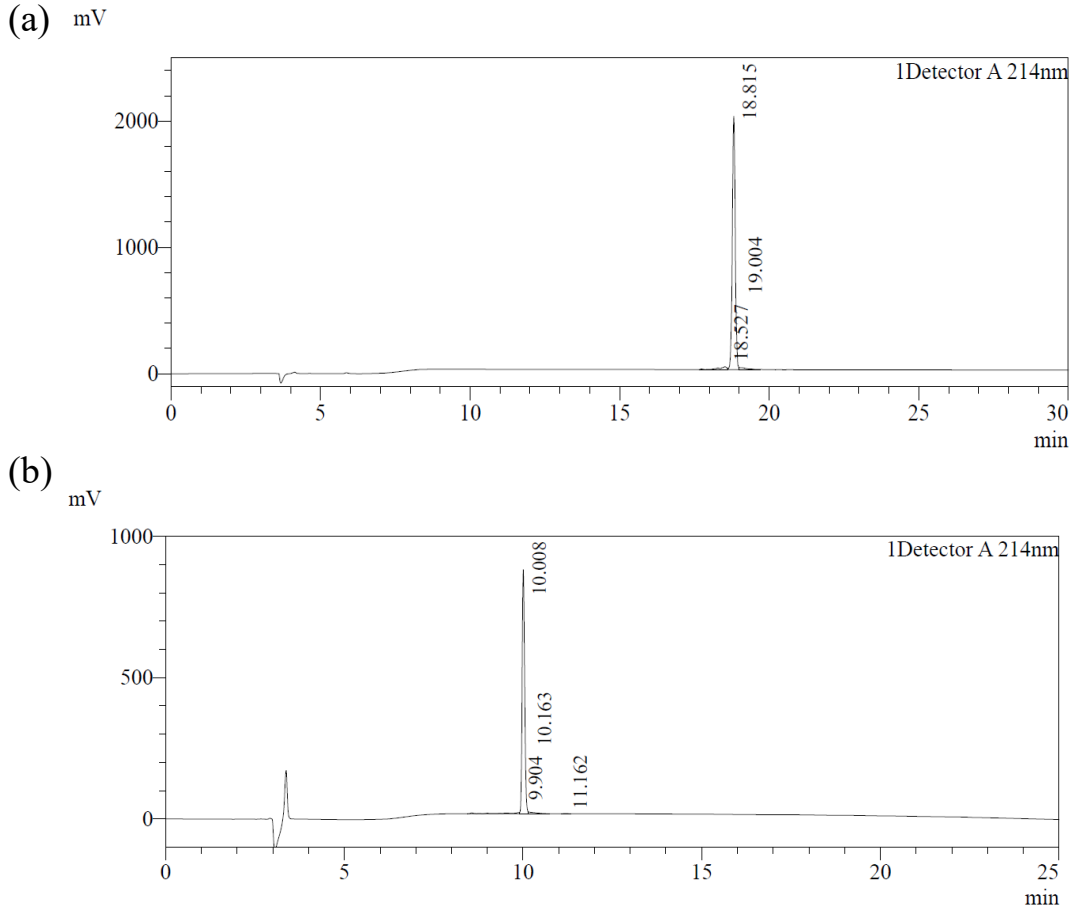

Figure S5. Typical HPLC chromatograms of (a) **NucCR** and (b) **NucCR'**, monitored at 214 nm.

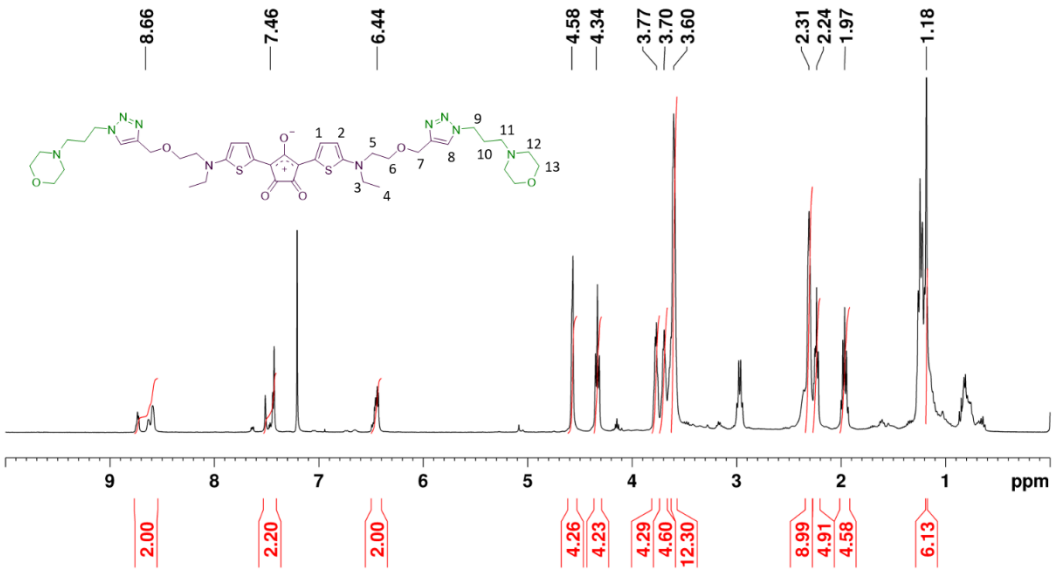

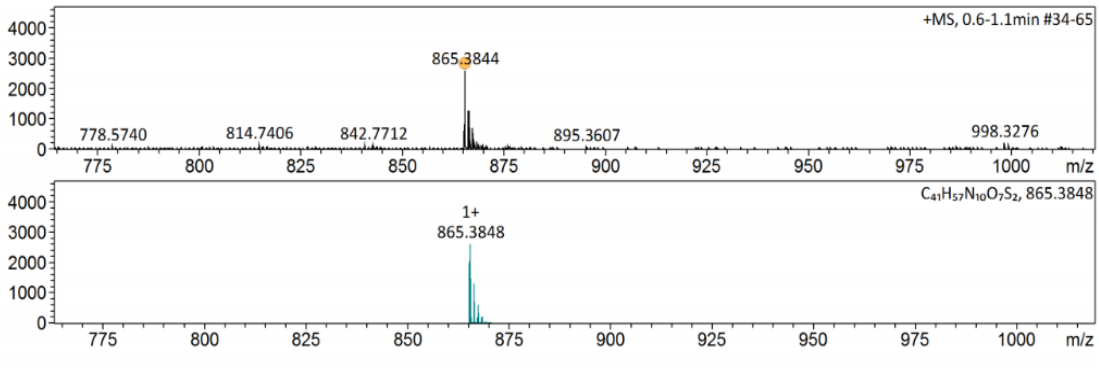

Meas. m/z	#	Ion Formula	m/z	err [ppm]	Mean err [ppm]	rdb	N-Rule	e⁻ Conf
865.384350	1	C41H57N10O7S2	865.384763	0.5	484.2	18.5	ok	even

Figure S6. ^{1}H NMR and HR-MS of **LysoCR**. Note that the ^{1}H NMR shows peaks for three conformational croconaine isomers.[S1]

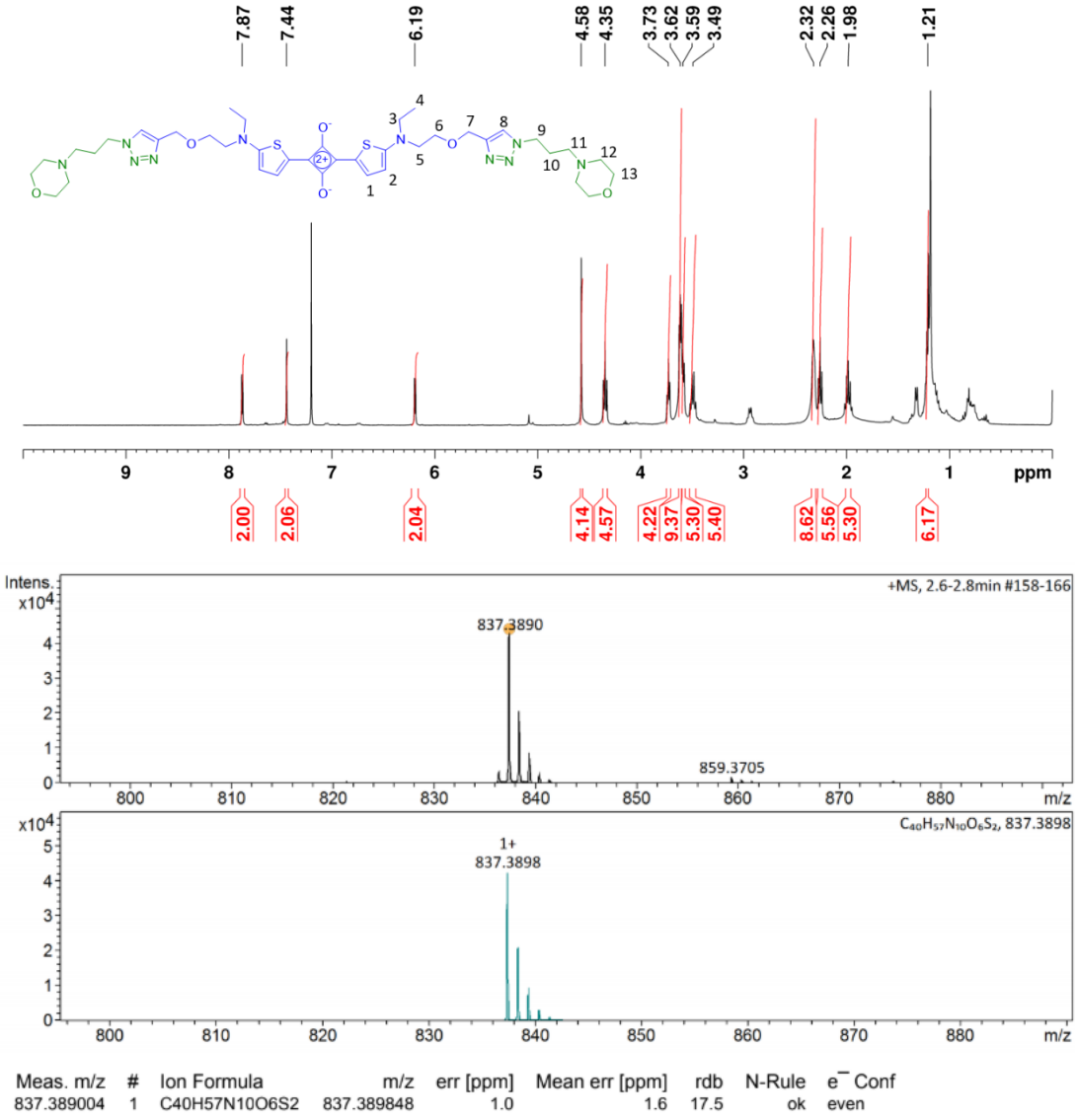

Meas. m/z	#	Ion Formula	m/z	err [ppm]	Mean err [ppm]	rdb	N-Rule	e⁻ Conf
837.389004	1	C40H57N10O6S2	837.389848	1.0	1.6	17.5	ok	even

Figure S7. ^{1}H NMR and HR-MS of **LysoSQ**.

3. Absorption and Fluorescence Spectra

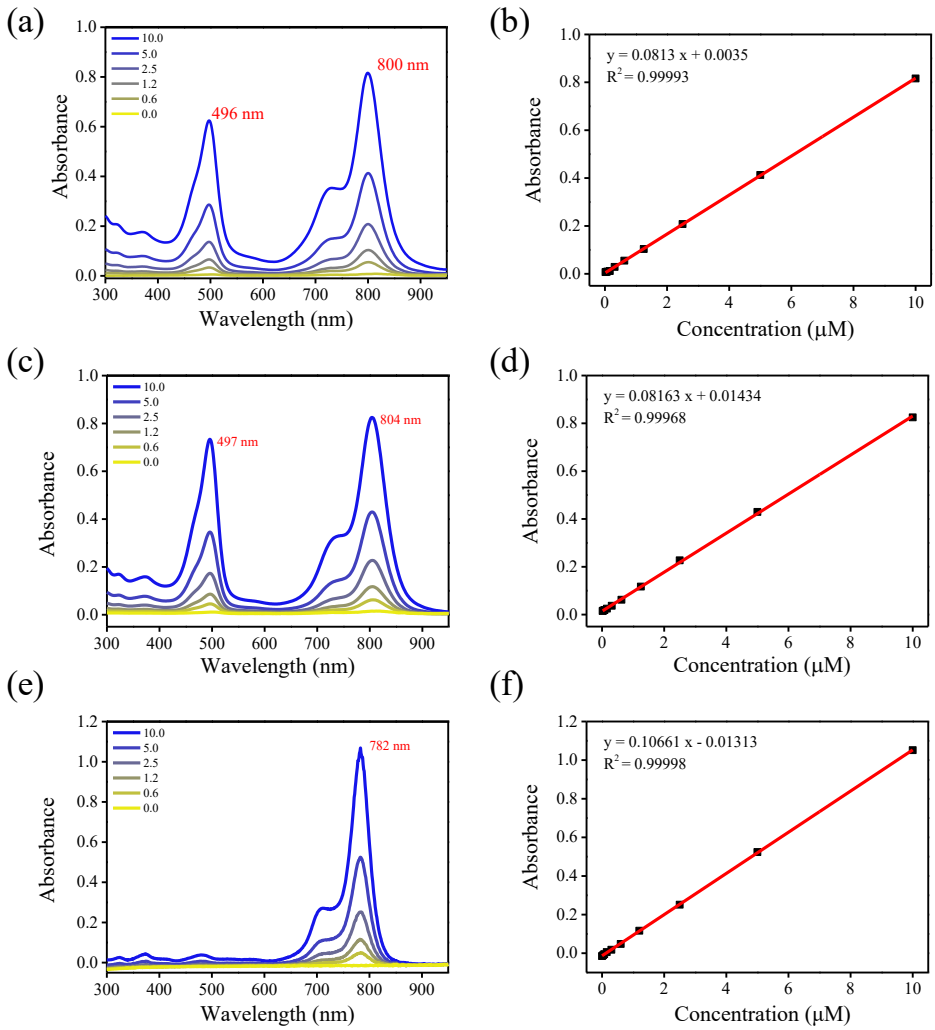

Figure S8. Absorption spectra of (a) **NucCR**, (c) **NucCR'** and (e) **LysoCR** at different concentrations in PBS solution (1% DMSO, pH 7.2). Linear relationship of absorbance for the maxima peak versus concentration for (b) **NucCR**, (d) **NucCR'** and (f) **LysoCR**.

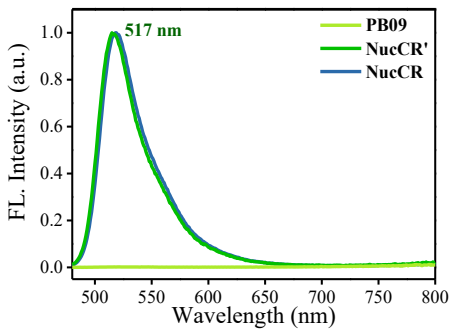

Figure S9. Fluorescence spectra of 5 μM **PB09**, **NucCR** and **NucCR'** in PBS solution (1% DMSO, pH 7.2). λ_{ex} = 460 nm. Slit: 2.5 nm/2.5 nm.

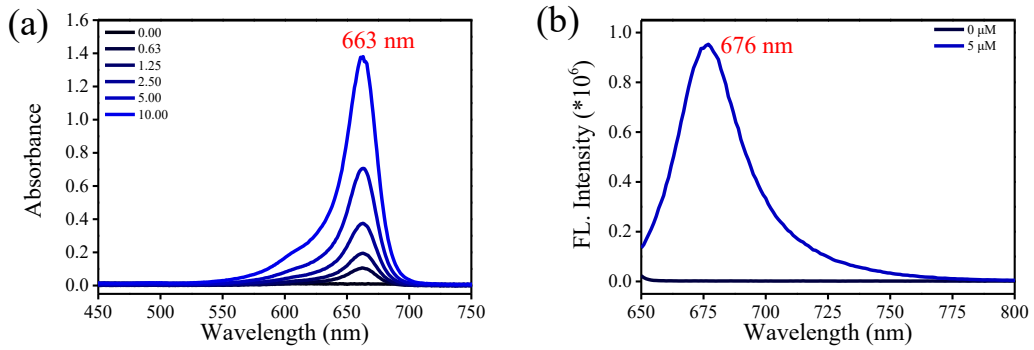

Figure S10. (a) Absorption and (b) fluorescence spectra of **LysoSQ** in PBS solution (1% DMSO, pH 7.2). λ_{ex} = 640 nm. Slit: 2.5 nm/2.5 nm.

4. Photothermal Experiments

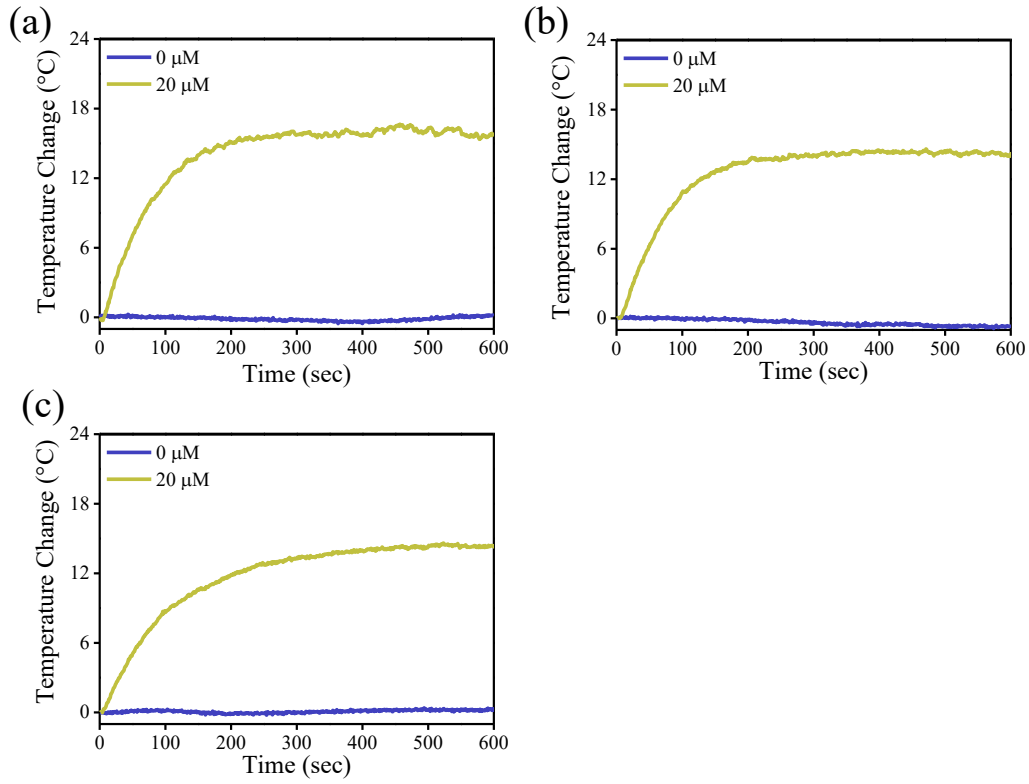

Figure S11. Change in temperature within the spot of the laser beam (see Figure S12 for illustration) for samples of (a) **NucCR**, (b) **NucCR'** and (c) **LysoCR** in PBS solution (pH 7.2, 4% DMSO) over time, upon the irradiation at 808 nm with 5.0 W/cm^2.

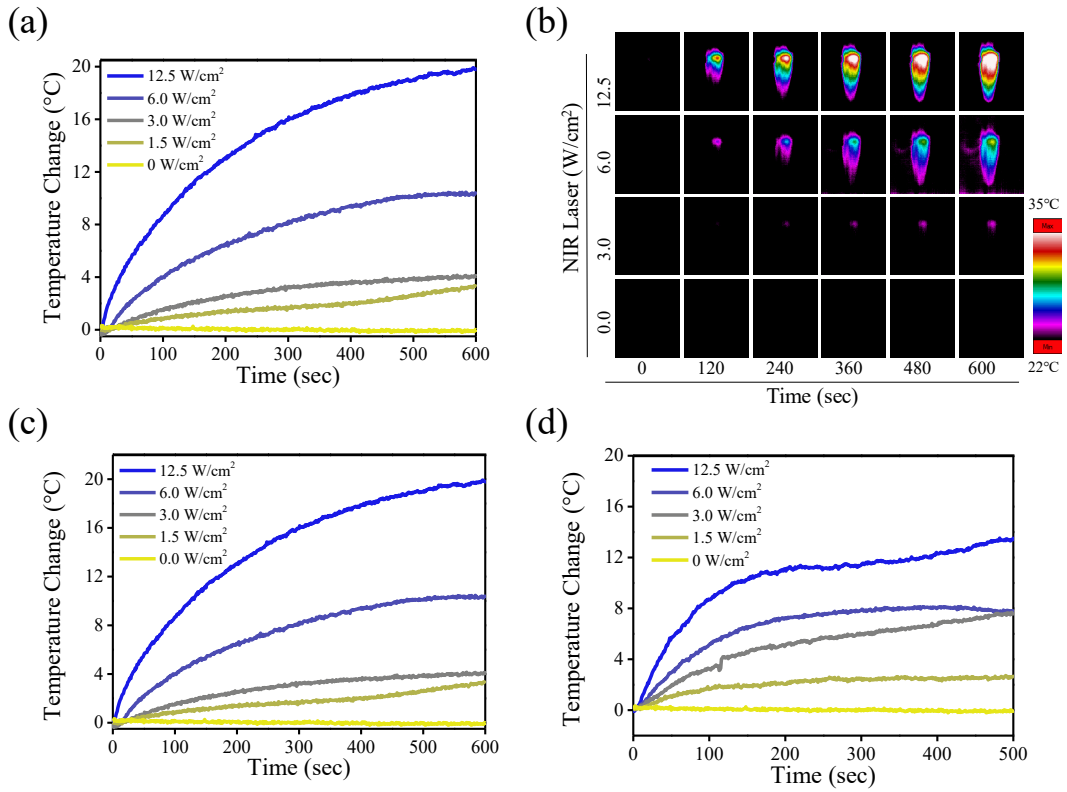

Figure S12. Change in temperature with time upon irradiation of 10 μM (a) **NucCR**, (c) **NucCR'** and (d) **LysoCR** with an 808 nm laser at different power densities. (b) Corresponding thermal images of the **NucCR** aqueous solution under laser irradiation.

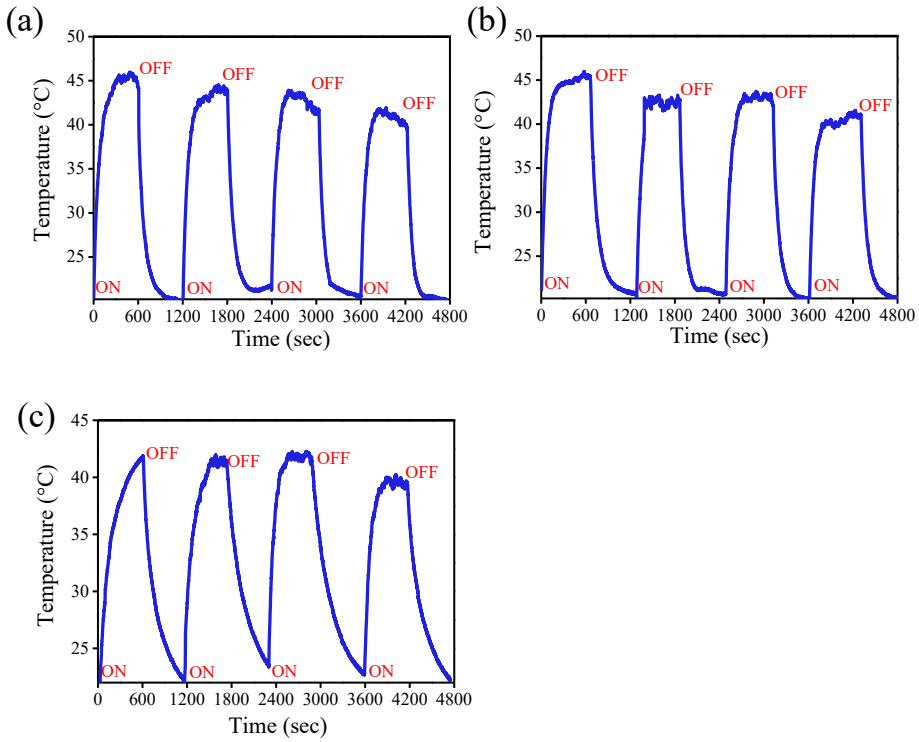

Figure S13. Four heating cycles of 100 μM (a) **NucCR**, (b) **NucCR'** and (c) **LysoCR** in PBS solution (pH 7.2, 4% DMSO) with laser irradiation at 808 nm (5 W/cm^2).

Table S1. The photothermal behavior of organic dyes reported in the last two years

Probe Construction	Organelle target	Laser irradiation	Photothermal effect	Refs
Micelles loaded with cyanine dye	Mitochondria	635 nm, 0.5 W/cm^2, 10 min	Increase by ~27 ℃ (H_2O, 500 μM)	S4
Nanoparticles encapsulated by BODIPY dye	-	808 nm, 0.3 W/cm^2, 5 min	Increase by ~54 ℃ (H_2O, 25 μM)	S5
Nanoparticles self-assembled from quaterrylenediimide derivative	-	808 nm, 1 W/cm^2, 5 min	Increase to 62 ℃ (PBS, 150 μg/mL)	S6
Nanoparticles loaded with donor-acceptor conjugated small molecule	-	808 nm, 0.8 W/cm^2, 5 min	Increase by 54 ℃ (PBS, 100 μM)	S7
Phthalocyanine dyes (example as **PcA1**[8])	-	730 nm, 1.0 W/cm^2, 10 min	Increase by ~20 ℃ (H_2O/0.1% Cremophor EL, 10 μM)	S8
IR-1048 dye triggered by hypoxia	-	980 nm, 0.1 W/cm^2, 2 min	Increase by 27 ℃ (HEPES, 5 μg/mL)	S9
Nanoparticles assembled with human serum albumin and phenazine-cyanine dyes (example as **PH-2@HSA**[10])	-	808 nm, 1 W/cm^2, 5 min	Increase to 53 ℃ (PBS, 20 μM)	S10
Nanoparticles assembled from porphyrin-diketopyrrolopyrrole derivatives	-	808 nm, 1 W/cm^2, 10 min	Increase to 50 ℃ (H_2O, 80 μg/mL)	S11
Nanoparticles loaded with small organic molecule as electron-deficient thiadiazolobenzotriazole core	-	808 nm, 2 W/cm^2, 5 min	Increase to 66 ℃ (PBS, 50 μg/mL)	S12
Nanoparticles assembled from cruciform phthalocyanine pentad dye		1064 nm, 0.9 W/cm^2, 10 min	Increase by 24 ℃ (H_2O, 27 ppm)	S13
Nanoparticles assembled from acceptor–donor–acceptor structured small molecule		660 nm, 1 W/cm^2, 10 min	Increase by ~35 ℃ (PBS, 40 μg/mL)	S14
Croconaine dyes	**Nucleus Lysosome**	**808 nm, 5 W/cm^2, 10 min**	**Increase by 16 ℃ (NucCR), 14 ℃ (NucCR'), 14 ℃ (LysoCR), (PBS, 20 μM)**	**This work**

5. Croconaine Stability Tests

Before initiating cell studies, it was important to establish that the probes were chemically stable under conditions that mimic the intracellular environment. The primary concern was possible susceptibility of the squaraine and croconaine chromophores to chemical bleaching due to nucleophilic attack by biological thiols, especially glutathione (GSH), cysteine (Cys) or homocysteine (Hcy).[S15–18] Thus, cuvette studies were conducted that monitored the change in absorption and fluorescence of **NucCR** and **NucCR'** in the presence of 10 mM GSH, the most abundant cellular thiol. As shown in Figure S14 the croconaine absorbance did not change over 30 minutes. Additional experiments tested the stability of **LysoCR** and **LysoSQ** in the presence of an excess of GSH, Cys or Hcy, and also observed no change in absorption over 30 min (Figure S15). Also included in the Figure S15 is the result of a control experiment showing that the thiols quickly attacked and bleached the more reactive squaraine dye **ConSQ** whose structure has two 4-aminophenyl rings and thus has a more electrophilic core. This comparison shows that the two strongly electron donating 2-aminothiophene rings within the structures of **LysoCR** and **LysoSQ** are able to greatly reduce the electrophilicity of the central cyclic core in each chromophore such that they resist nucleophilic attack when inside cells.[S1] Taken together, the photothermal heating and stability studies strongly indicate that **NucCR**, **NucCR'** and **LysoCR** are all excellent candidates for photothermal heating inside cells.

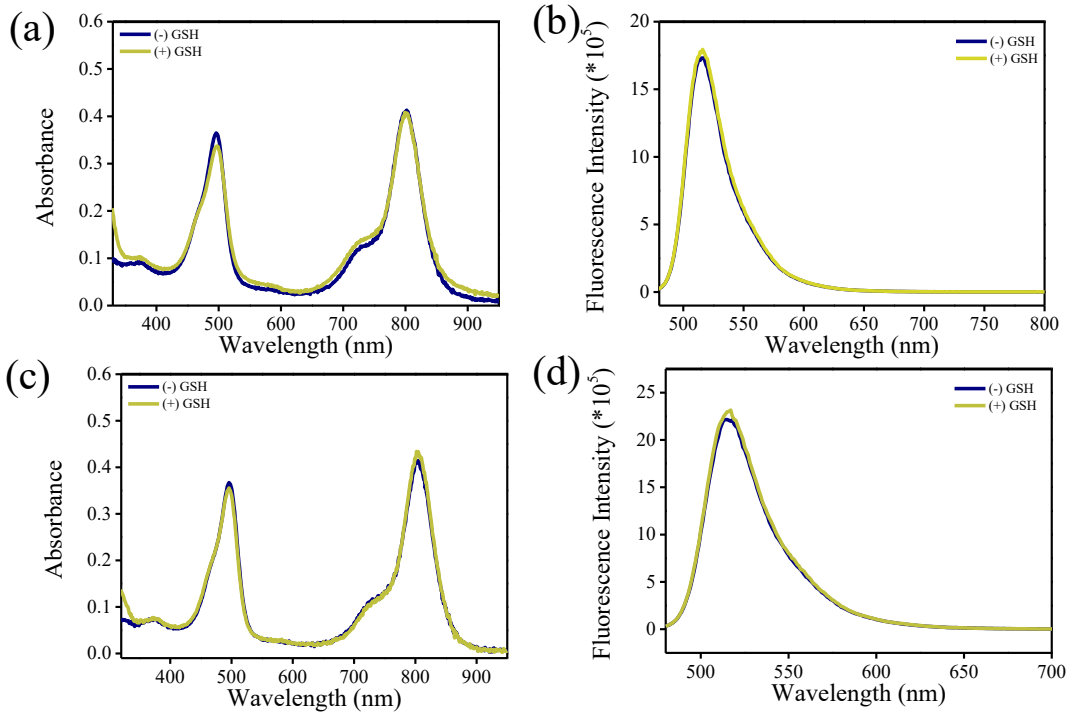

Figure S14. (a, c) Absorption and (b, d) fluorescence spectra of 5 μM (a, b) **NucCR** or (c, d) **NucCR'** in 100 mM potassium phosphate buffer (1%DMSO, pH 7.4) without or with 10 mM GSH for 30 min, λ_{ex} = 470 nm. Slit: 2.5 nm/2.5 nm.

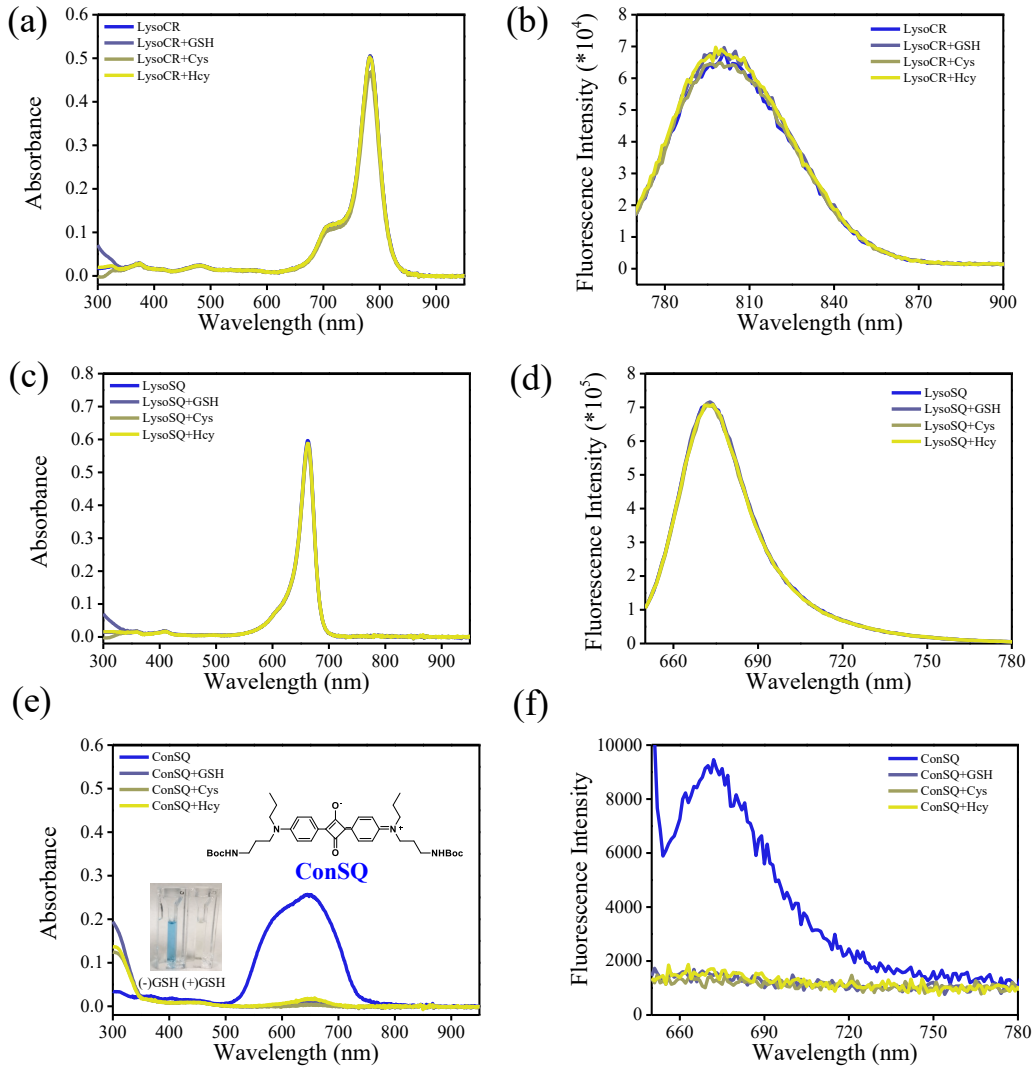

Figure S15. (a, c, e) Absorption and (b, d, f) fluorescence spectra of 5 μM (a, b) **LysoCR** or (c, d) **LysoSQ** or (e, f) **ConSQ** in 100 mM potassium phosphate buffer (1% DMSO, pH 7.4) without/with 10 mM GSH, Cys or Hcy for 30 min. (b, f) λ_{ex} = 640 nm. Slit: 2.5 nm/2.5 nm. (d) λ_{ex} = 750 nm. Slit: 5 nm/5 nm.

6. Fluorescence Microscopy Data

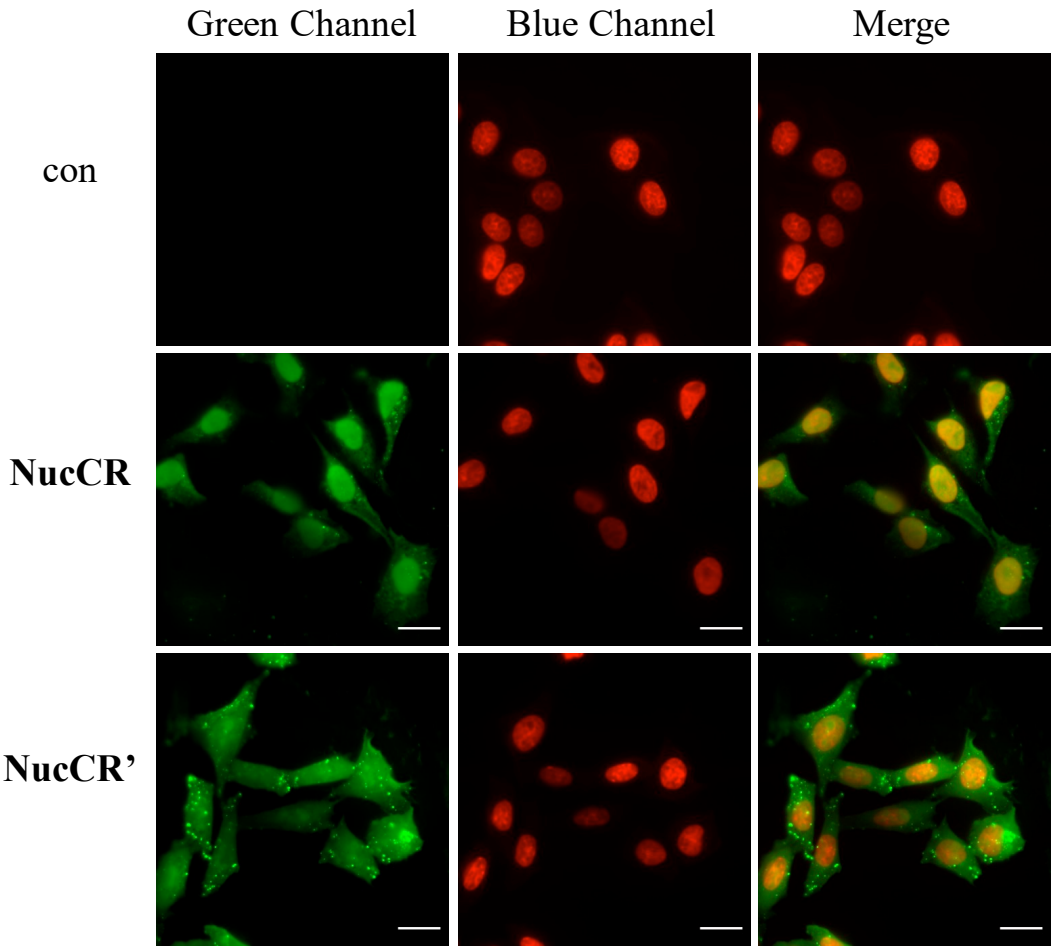

Figure S16. Distribution of **NucCR** or **NucCR'** in CHO-K1 cells. Fluorescence images of CHO-K1 cells sequentially incubated with 10 μM **NucCR** or **NucCR'** for 2 h, followed by 3 μM Hoechst 33342 for 15 min. Cells in con group were treated only with Hoechst. Green channel for **NucCR** or **NucCR'**, ex. 450/90 nm, em. 500/50 nm; Blue channel for Hoechst 33342, ex. 387/11 nm, em. 447/60 nm. Scale bar = 20 μm.

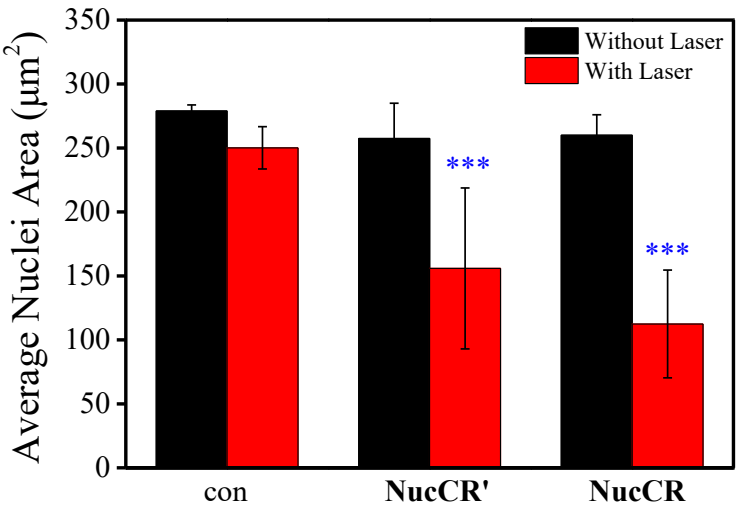

Figure S17. Quantification of average nuclei area of MCF-7 cells after photothermal treatment. Cells were treated with 50 μM **NucCR** or **NucCR'** for 2 h, replaced by fresh medium and irradiated with an 808 nm laser (5 W/cm^2, 10 min), and stained with 3 μM Hoechst 33342 for 15 min. Micrographs (N = 3) were examined by ImageJ software to obtain average values for nuclei area. The threshold *p*-values are: *** $p < 0.001$.

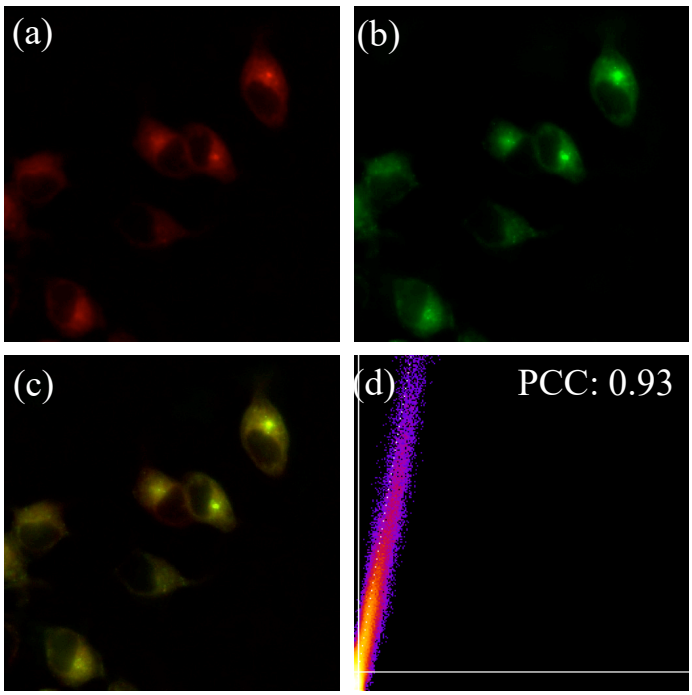

Figure S18. Distribution of **LysoSQ** in MCF-7 cells. Fluorescence images of MCF-7 cells co-incubated with 10 μM **LysoSQ** for 2 h, and Lysotracker Yellow for 30 min. (a) Deep red channel for **LysoSQ**, ex. 655/40 nm, em. 716/40 nm; (b) Green channel for Lysotracker Yellow, ex. 450/90 nm, em. 500/50 nm; (c) Merge images of (a) and (b); (d) The correlation of **LysoSQ** and Lysotracker Yellow intensities.

7. References

S1 G. T. Spence, G. V. Hartland and B. D. Smith, *Chem. Sci.*, 2013, **4**, 4240–4244.

S2 E. M. Peck, W. Liu, G. T. Spence, S. K. Shaw, A. P. Davis, H. Destecroix and B. D. Smith, *J. Am. Chem. Soc.*, 2015, **137**, 8668–8671.

S3 Y. Wen, K. Liu, H. Yang, Y. Li, H. Lan, Y. Liu, X. Zhang and T. Yi, *Anal. Chem.*, 2014, **86**, 9970–9976.

S4 H. Wang, J. Chang, M. Shi, W. Pan, N. Li and B. Tang, *Angew. Chem. Int. Ed.*, 2019, **58**, 1057–1061.

S5 D. Xi, M. Xiao, J. Cao, L. Zhao, N. Xu, S. Long, J. Fan, K. Shao, W. Sun, X. Yan and X. Peng, *Adv. Mater.*, 2020, **32**, 1–8.

S6 C. Liu, S. Zhang, J. Li, J. Wei, K. Müllen and M. Yin, *Angew. Chem.Int. Ed.*, 2019, **58**, 1638–1642.

S7 S. Liu, X. Zhou, H. Zhang, H. Ou, J. W. Y. Lam, Y. Liu, L. Shi, D. Ding and B. Z. Tang, *J. Am. Chem. Soc.*, 2019, **141**, 5359–5368.

S8 X. Li, X. H. Peng, B. De Zheng, J. Tang, Y. Zhao, B. Y. Zheng, M. R. Ke and J. D. Huang, *Chem. Sci.*, 2018, **9**, 2098–2104.

S9 X. Meng, J. Zhang, Z. Sun, L. Zhou, G. Deng, S. Li, W. Li, P. Gong and L. Cai, *Theranostics*, 2018, **8**, 6025–6034.

S10 Y. Yan, J. Chen, Z. Yang, X. Zhang, Z. Liu and J. Hua, *J. Mater. Chem. B*, 2018, **6**, 7420–7426.

S11 F. Wu, L. Chen, L. Yue, K. Wang, K. Cheng, J. Chen, X. Luo and T. Zhang, *ACS Appl. Mater. Interfaces*, 2019, **11**, 21408–21416.

S12 B. Guo, Z. Huang, Q. Shi, E. Middha, S. Xu, L. Li, M. Wu, J. Jiang, Q. Hu, Z. Fu and B. Liu, *Adv. Funct. Mater.*, 2020, **30**, 1–11.

S13 H. Pan, S. Li, J. L. Kan, L. Gong, C. Lin, W. Liu, D. Qi, K. Wang, X. Yan and J. Jiang, *Chem. Sci.*, 2019, **10**, 8246–8252.

S14 Y. Cai, Z. Wei, C. Song, C. Tang, X. Huang, Q. Hu, X. Dong and W. Han, *Chem. Commun.*, 2019, **55**, 8967–8970.

S15 G. Saranya, P. Anees, M. M. Joseph, K. K. Maiti and A. Ajayaghosh, *Chem- A Eur. J.*, 2017, **23**, 7191–7195.

S16 L. Tang, F. Yu, B. Tang, Z. Yang, W. Fan, M. Zhang, Z. Wang, O. Jacobson, Z. Zhou, L. Li, Y. Liu, D. O. Kiesewetter, W. Tang, L. He, Y. Ma, G. Niu, X. Zhang and X. Chen, *ACS Appl. Mater. Interfaces*, 2019, **11**, 27558–27567.

S17 P. Anees, S. Sreejith and A. Ajayaghosh, *J. Am. Chem. Soc.*, 2014, **136**, 13233–13239.

S18 K. V. Sudheesh, M. M. Joseph, D. S. Philips, A. Samanta, K. Kumar Maiti and A. Ajayaghosh, *ChemistrySelect*, 2018, **3**, 2416–2422.